NON-DESTRUCTIVE ANALYSIS BY SMALL ANGLE NEUTRON SCATTERING

P. Bianchi°, F. Carsughi*, D. D'Angelo°, M. Magnani*, A. Olchini°,

M. Stefanon*, and F. Rustichelli*

°C.R.T.N. ENEL, Milano, Italy

*E.N.E.A., Bologna Italy

*Istituto di Fisca Medica, Universita di Ancona, Italy

Abstract

An investigation of service effects on the Ni-based superalloy UDIMET® 720 was performed by using Small Angle Neutron Scattering (SANS). In particular, gamma prime precipitate evolution was considered. The investigated sample was obtained from a turbine blade used in a turbogas power plant where the working temperature was about 850°C. Transmission Electron Microscopy (TEM) observations were compared to SANS data, which were obtained at D11 Diffractometer at ILL in Grenoble (France). The SANS theory allowed the determination of useful microstructural information, such as the volume fraction, the correlation length (which gives an idea of the packing of the system), and the Particle Size Distribution (PSD) of the precipitates. A comparison with as-heat-treated turbine blades showed the evolution of the microstructure of the superalloy during its operating life. In conclusion, SANS is a powerful non-destructive technique, which could be routinely employed to appraise the condition of materials used in technological applications.

Superalloys 1988
Edited by S. Reichman, D.N. Duhl,
G. Maurer, S. Antolovich and C. Lund
The Metallurgical Society, 1988

Introduction

The main aims of research and development related to advanced materials for elevated temperature applications in electrical energy production are the optimization of power plant efficiency and component availability.

These aims could generally be pursued by means of comprehensive control of material behavior during component operation life. Such action should be split up into a wide characterization of the mechanical properties of the material to be considered at the design stage, as well as a reasonable description of the material response to the in-service damage phenomena.

To pursue the double purpose of better design and reliable operation, it is advisable to extend the microstructural assessment of new and service-exposed materials and to introduce advanced non-destructive diagnostic techniques, respectively.

With respect to this approach, attention has been focused on UDIMET 720, a Ni-based superalloy for power plant gas turbine blade applications. An investigation of thermal mechanical treatment effects was performed by using Small Angle Neutron Scattering (SANS) to analyze the precipitation evolution during the operation life.

SANS technique, which is non-destructive on small components, allows the quantitative determination of relative microstructural parameters such as precipitation, dislocation and cavitation, in a precise, reproducible and efficient manner as discussed in Ref. 1, where some of these investigations on superalloys are reported.

To calibrate the figures obtained by the SANS method, a metallographical survey was performed by scanning (SEM) and transmission (TEM) electron microscopes.

Materials

Nickel-based superalloys are widely used in high temperature applications. UDIMET 720 has been developed for this purpose and, in particular, is used for turbine blades of turbogas power plants, where the material working temperature is about 850°C.

The nominal composition (wt%) of the alloy is:

Ni	56.10
Co	14.00
Mo	3.00
W	1.30
Cr	17.20
Al	2.50
Ti	4.80
C	0.035
B	0.035
Fe	0.16
Si	0.2

and gamma prime phase precipitation hardening occurs to increase heat resistance.

The material consists of a gamma phase matrix with a bimodal distribution of gamma prime precipitates. In particular, the primary gamma prime

phase is larger in size and cuboidal in shape, while the secondary gamma prime is smaller in size and spherical in form.

Three different UDIMET 720 samples have been investigated in order to reveal thermomechanical effects on the microstructure. First, an un-heat-treated sample was studied for the presence of precipitates due to solidification. Also, an as-heat-treated sample, taken from a virgin turbine blade, was investigated to show the wide precipitation induced by the heat treatment. Finally, a post-service turbine blade was considered in order to investigate the damage produced during service.

The operation time was 8000 hours at a maximum metal temperature of 850°C with thermal gradients and thermal fatigue. In combination with the presence of combustion gases, it produced a high stress field inside the turbine blade accompanied by corrosive attack.

Microstructural Characterization

The as-heat-treated sample's microstructure has been investigated by light, electron scanning, and transmission microscopy techniques; the results are presented in Ref. 2 and 3.

By the same method, the post-service sample has been studied in order to show microstructural changes in comparison with other samples.

Such material shows an equiaxed grain structure, where the grain dimensions are about doubled compared with those of the as-heat-treated turbine blades.

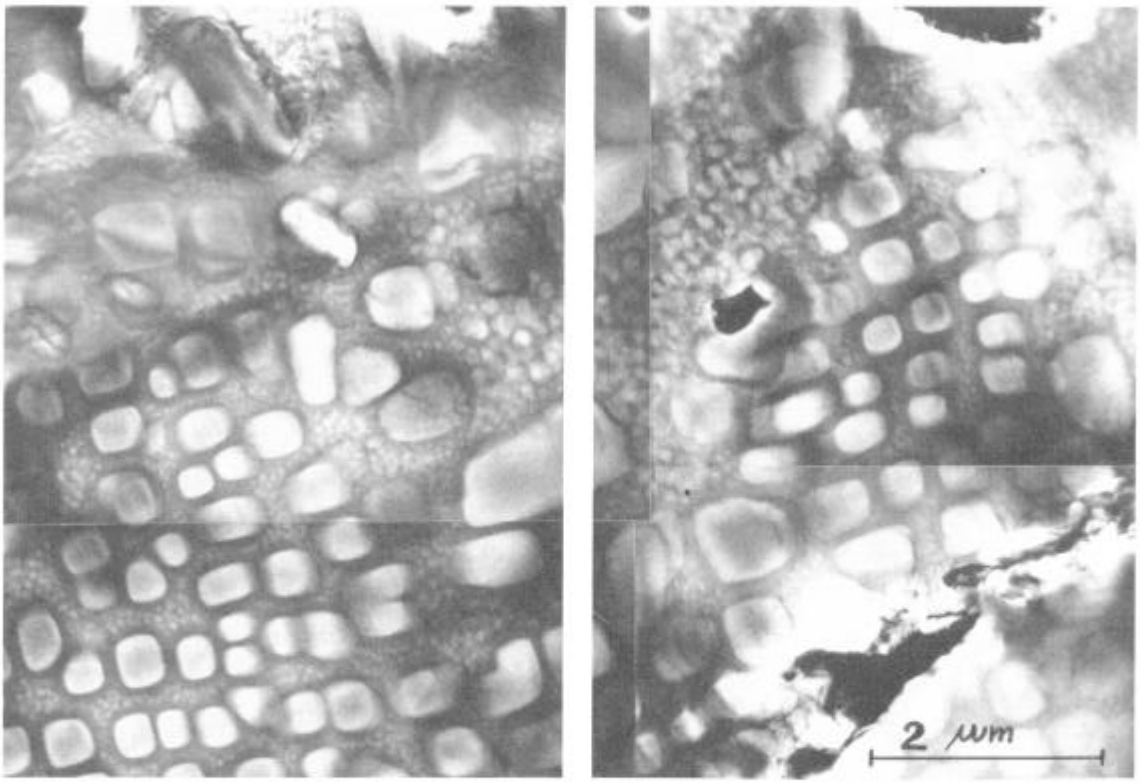

Figure 1 - TEM observations of primary and secondary gamma prime precipitation of the as-heat-treated turbine blade.

Both gamma and gamma prime phases have an FCC lattice with cell dimensions of 0.3524 nm and 0.3600 nm, respectively. Gamma prime particles show

a cuboidal and globular shape for primary and secondary precipitates, respectively (Fig. 1).

Secondary gamma prime precipitates, with a dimension of the order of magnitude between 10^1 and 10^2 nm, have been detected.

Grain boundaries are subjected to recrystallization and subgrain nucleation occurs, especially when the gamma prime primary precipitates are drawn out into a radial crown morphology (Fig. 2).

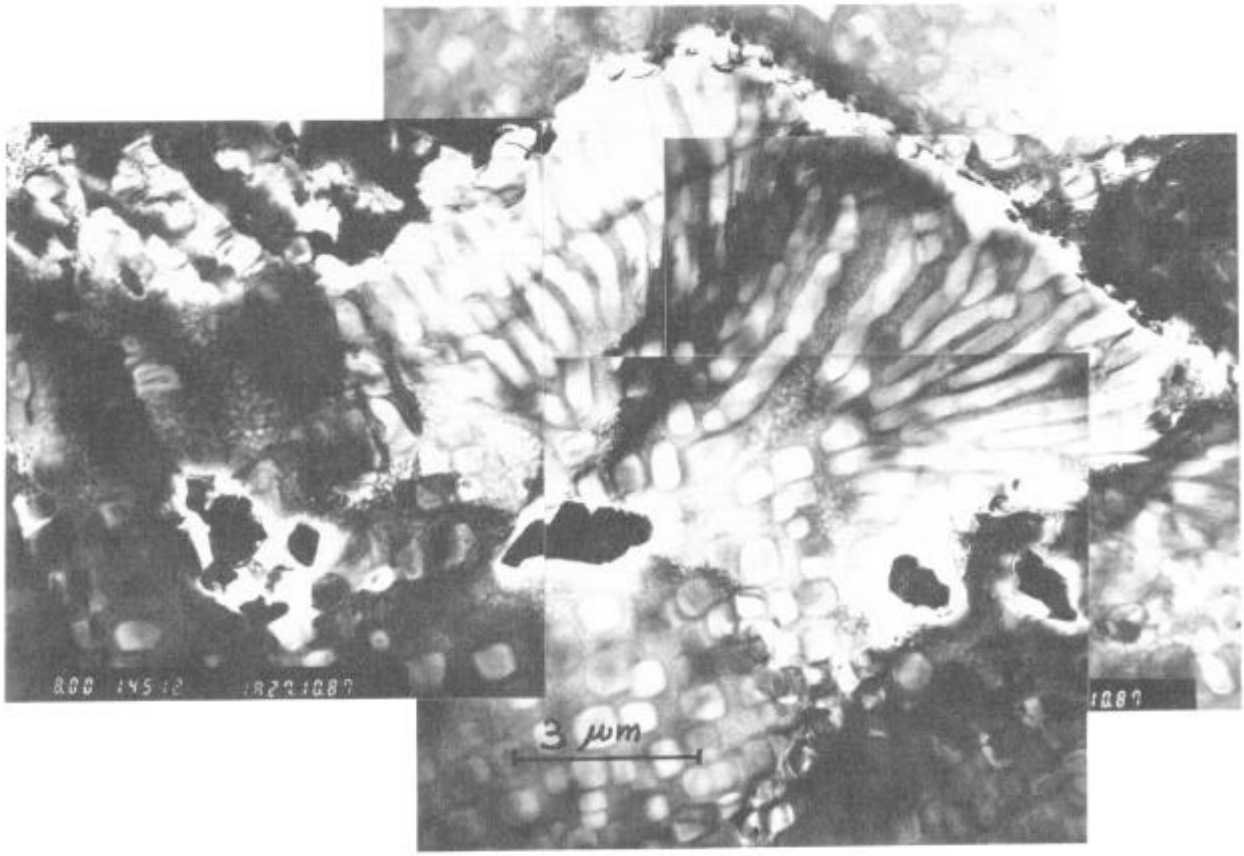

Figure 2 - Gamma prime precipitation close to grain boundaries where recrystallization processes occur in the post-service turbine blade.

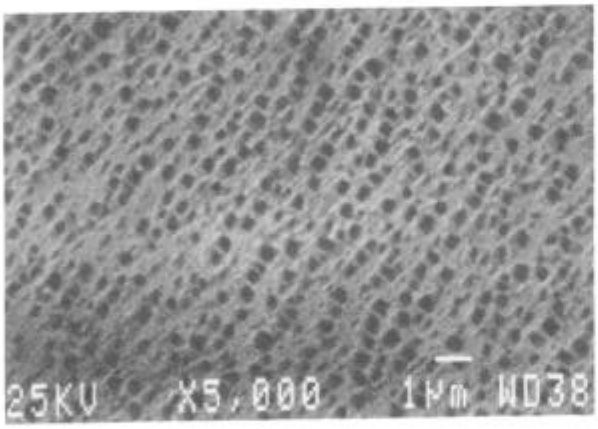

Figure 3 - Gamma prime precipitation inside the "normal" matrix of the post-service turbine blade

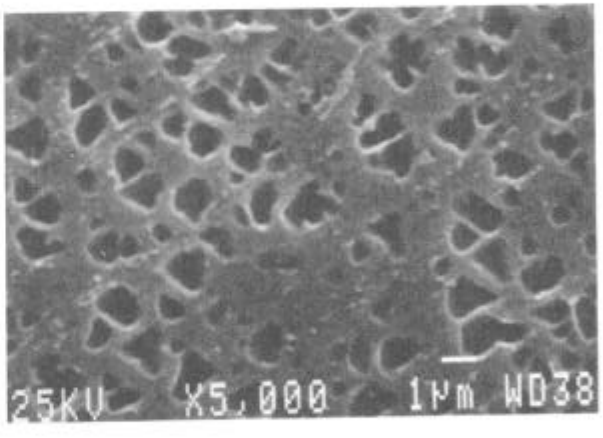

Figure 4 - Gamma prime precipitation inside the "islands" in the matrix of the post - service turbine blade.

The most evident change induced in the microstructure of UDIMET 720 during operation is the presence of wide "islands" where the gamma prime primary precipitates have larger dimensions, up to 0.8 μm, while inside the "normal" matrix, the gamma prime dimensions are at a maximum of about 0.3 μm (Figs. 3-4).

The mechanism of the gamma prime dimensional increase seems to be due to single particle growing related to multiple coalescence.

SANS Theoretical Introduction

When incident radiation strikes material containing inhomogeneities with dimensions up to two or three orders of magnitude larger than the radiation wavelength, the so-called Small Angle Scattering phenomenon occurs. The outcoming wave presents a maximum at the same direction of the incident wave and decreases very quickly when larger angles are observed.

With K the wave vector, and i, o indices of the Incident and Outcoming wave front, we can define an EXCHANGED WAVE VECTOR, Q, by:

$$Q = K_i - K_o \tag{1}$$

Where the wave vector, K, is related to the wavelength by:

$$K = 2\pi/\lambda \tag{2}$$

As in the small angle scattering technique, elastic scattering is considered (one that has $K_o = K_i$). Under these conditions, by simple geometrical considerations, it is possible to equate Q with the scattering angle, 2Θ, and the wavelength of incident radiation by:

$$Q = \frac{4\pi}{\lambda} \sin \Theta \tag{3}$$

The outcoming wavefront drops to zero when:

$$2\Theta = \frac{\lambda}{D} \tag{4}$$

where D is the dimension of the scattering inhomogeneities.

It is clear that the precipitated phases inside a matrix play the role of the previous scattering inhomogeneities. Small Angle Neutron Scattering (SANS) offers, in metallurgical application, a powerful method which can be used to investigate important elements of the microstructure such as magnetic domain, precipitated phases, and microvoids produced by creep, fatigue and irradiation. The dimension of the scattering particles are connected to the Q range to be investigated by:

$$Q \cdot D \approx 2\pi \tag{5}$$

The formal theory of SANS is beyond the aim of this work but, if we consider the simplified model of a two-phase material, it is possible to develop some important relationships between the experimental data and the scattering particle parameters.

During an experiment, we can measure the coherent macroscopic cross section $d\Sigma/d\Omega(Q)$ that we call the scattering curve or function, whose properties will be discussed in the next section.

The use of a neutron beam allows the investigation of samples whose thickness is of the order of a cm, because:

$$\Sigma_t = \frac{1}{L} \tag{6}$$

where L is the free mean path of neutrons inside the sample and Σ_t is the total neutron cross section taking into account both absorption and scattering phenomena.

Another kind of radiation could be used for the Small Angle Scattering experiment but, due to the high interaction of electrons or X-ray, the thickness of samples in these cases must be very thin to avoid total absorption by the sample.

As a consequence, it is clear that a nondestructive test is possible only if a neutron beam is used.

Scattering Function and Its Properties

The interaction between the neutrons and the investigated sample depends upon the difference of the scattering length density, ρ_b, between the two phases: the precipitates and the matrix.

Since p and m indices are related to the precipitates and matrix, the SANS theory shows that, if we consider a set of N_p identical particles, the scattering function is:

$$\frac{d\Sigma}{d\Omega}(Q)=(\Delta\rho)^2 \cdot N_p V_p^2 \left|F_p(Q,R)\right|^2 \tag{7}$$

when

$$(\Delta\rho) = \rho_{bp} - \rho_{bm} \tag{8}$$

where $F_p(Q,R)$ is the form factor of a single particle whose volume is V_p, depending upon its form and dimension, R.

Guinier approximation

It has been shown that it is possible to connect the scattering curve to a Giration Radius, R_g, of the particle, depending upon the form and dimension, D.

In particular, for small values of the product Q·D (for example, for spherical shape, this approximation holds for Q·R<1.2), is:

$$\left|F_p(Q,R)\right|^2 \alpha \exp(-Q^2R_g^2/3) \tag{9}$$

the value of R_g is the slope of the straight line fitting the experimental data in the $Ln(d\Sigma/d\Omega)$ vs Q^2 plane; if a sphere has a radius R_s, the giration radius is:

$$R_g = \sqrt{(3/5)}R_s \tag{10}$$

Porod approximation

In the case of well defined outlines of the scattering particles, Porod

has shown that the asymptotic value of the scattering function is:

$$\frac{d\Sigma}{d\Omega} = (\Delta\rho)^2 \cdot \frac{2\pi}{Q^4} \cdot S_p \qquad (11)$$

where S_p is the total surface of the particles per unit volume.

To verify if the asymptotic value has been reached, a check of this law is necessary. The plot of the scattering curve in the $\mathrm{Log}(d\Sigma/d\Omega)$ vs the $\mathrm{Log}Q$ plane must be approximated, at high values, by a straight line whose slope is -4.

Volume fraction

In the case of isotropic scattering, it is possible to demonstrate that [1]:

$$\int_o^\infty Q^2 \frac{d\Sigma}{d\Omega} dQ = 2\pi^2 (\Delta\rho)^2 \cdot C_p \cdot (1-C_p) \qquad (12)$$

where, V being the investigated volume of the sample, the volume fraction C_p is:

$$C_p = \frac{N_p \cdot V_p}{V} \qquad (13)$$

Correlation length

When a material shows a wide precipitation (C_p>10%), the system is said to be not diluted, and a correlation length, L_o, is necessary to express the packing of the particles.

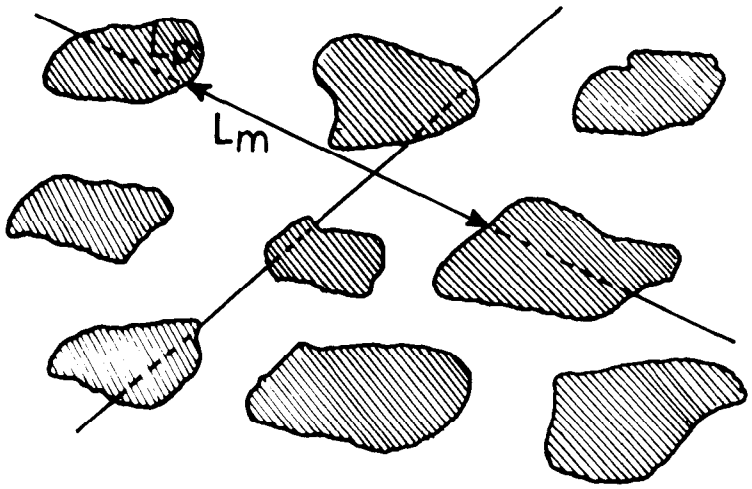

Figure 5 - The correlation length, L_o, depends upon the average particle dimensions, L_p, and on the average interparticle distances, L_m

L_m and L_p are the average chords for all directions between and through particles, respectively; L_o is defined by Fig. 5:

$$\frac{1}{L_o} = \frac{1}{L_p} + \frac{1}{L_m} \qquad (14)$$

and is connected to the scattering curve by [1]:

$$\int_0^\infty Q \frac{d\Sigma}{d\Omega} dQ = 2\pi \cdot (\Delta\rho)^2 \cdot L_o \cdot C_p \cdot (1-C_p) \qquad (15)$$

Particle size distribution

When the hypothesis of identical particles is not valid, the scattering curve is the superposition of scattering curves from each of the different particles.

In this case, it is very helpful to determine the particle size distribution, N(R), to characterize the polydisperse system.

It can be shown that:

$$\frac{d\Sigma}{d\Omega}(Q) = (\Delta\rho)^2 \cdot \int N(R) \cdot V^2_p(R) \cdot |F_p(Q,R)|^2 \, dR \qquad (16)$$

This relation holds when the different contributions add incoherently and the particles have a known shape.

In our analysis, we have fitted the scattering curve by a procedure that uses a constrained least-square calculation [6].

Experimental Technique

Our experiment was performed on D11 equipment at ILL in Grenoble, connected to the cold neutron source of the High Flux Reactor (HFR).

A neutron wavelength of 1 nm was used to avoid double Bragg and multiple scattering.

A simple vision of the experimental setup is shown in Fig. 6, where M is the monochromator; G's are the collimation guides; S is the sample position, and D is the dimensional detector.

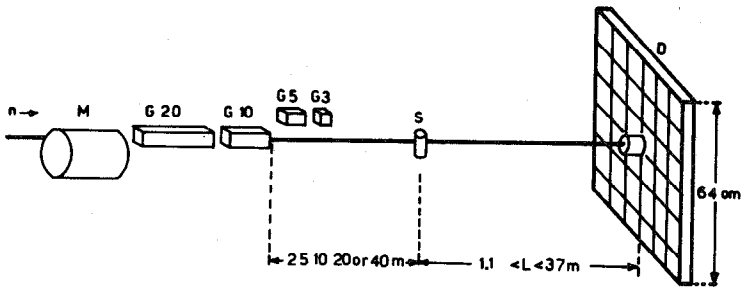

Figure 6 - Schematic view of the D11 Diffractometer

Different sample-detector distances were used to determine the investigated Q range by:

$$1.3 \cdot 10^{-2} < Q < 9 \cdot 10^{-1} \text{ nm}^{-1} \qquad (17)$$

which allows the investigation of particles whose dimensions, R, are included from 10 to 10^3 nm.

To determine the absolute value of the scattering curve, a calibration with a water sample was performed.

This calibration is necessary to bypass the measurements of important quantities like the neutron flux on the sample, the solid angle subtended by the detector and, at least, the detector efficiency [8].

Once we know the theoretical value of the incoherent scattering cross section of water, we can calculate the scattering curve by:

$$\frac{d\Sigma}{d\Omega}(Q) = \frac{d_w \cdot T_w}{d_s \cdot T_s} \cdot \frac{(I_s - b) - (T_s/T_h) \cdot (I_h - b)}{(I_w - b) - (T_w/T_q) \cdot (I_q - b)} \cdot (d\Sigma/d\Omega)w \qquad (18)$$

where d and T represent the thickness and the transmission factor, respectively; I and B the measured experimental intensities and the background, respectively; and w, s, h, and g are indices related to water, sample, sample holder and quartz cell, respectively.

Results and Discussion

The results concerning the evolution of the material microstructure relating to the thermal treatment have already been discussed in Ref. 2,3. In this work, only the microstructural evolution due to the operation is considered.

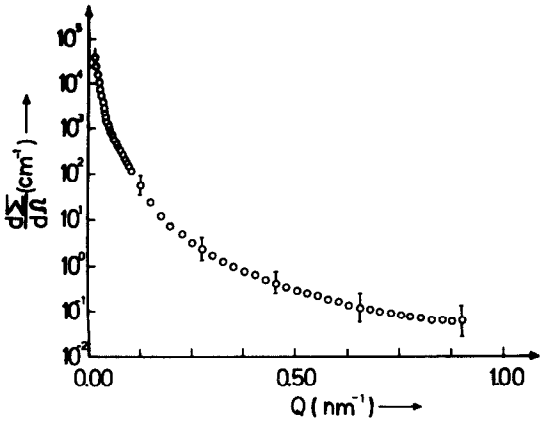

Figure 7 - Scattering pattern of the post-service turbine blade

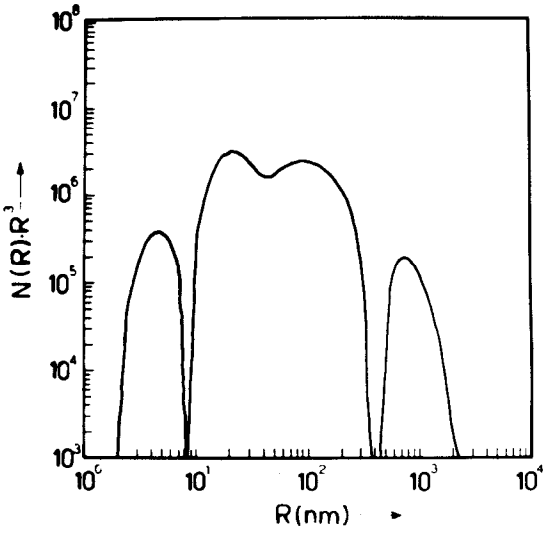

Figure 8 - Logarithmic volume size distribution of the post-service turbine blade

Fig. 7 shows the scattering pattern of the post-service turbine blade. The asymptotic behavior of the scattering curve does not have a perfect Q^{-4} dependence because the slope of the approximating straight line is about -3.2. This could be associated with scattering contribution due to very small particles (1 to 3 nm) or to a high dislocation density [1].

However, by the extrapolation by the Guinier law to Q=0, and by the Porod law to high Q values, the volume fraction and the correlation length have been obtained. A volume fraction of about 30% was found by equation 12, which is about the same as the value found for the new turbine, which was 35%. Moreover, the packing of the system is defined by the correlation length for which a value of 85 nm was found by equation 15, compared to 172 and 129 nm for the untreated and as-heat-treated samples, respectively.

These values give an idea of the different interparticle distance in the three samples. This is strictly connected to those islands found inside the matrix, where gamma prime precipitates are bigger and more packed than in other zones.

The particle size distribution obtained by a fitting procedure of the experimental data shows an increase in the dimension of the primary gamma prime particles and the presence of a new family of small particles (Fig. 8), whose average dimension is around 4 nm.

These particles could be related to microvoids produced by high stress fields inside the blade during operation, but this is not verified by TEM observations. In this case, the two-phase model would not be completely appropriate, and only a comparison with an unstressed, but thermally treated sample would allow the determination of the stress contribution to the damage of the material.

In conclusion, the importance of the Neutron Scattering technique in the field of non-destructive testing of materials is evident. For analyzing very thick samples, other phenomena, such as multiple scattering, have to be taken into account and refraction effects have to be considered.

An approximated elaboration of the SANS data, as it was performed in this and previous investigations on UDIMET 720, seems to provide, in a completely non-destructive manner, structural information in agreement with TEM observations, which are quite useful for operating applications.

References

1. H. Walther and P. Pizzi, Small Angle Neutron Scattering for Nondestructive Testing (New York, NY: Academic Press, 1980), 341.

2. P. Bianchi et al., "Non-Destructive Analysis of the Gamma Prime Precipitation in UDIMET 720 Ni Superalloy Turbine Blade by SANS," Material Science Forum, in print.

3. P. Bianchi et al., "Neutron Small Angle Scattering on UDIMET 720 Ni Superalloy Turbine Blade. Non-Destructive Analysis of the Gamma Prime Precipitation," Metallurgical Science and Technology, in print.

4. A. Guinier and J. Fournet, Small Angle Scattering of X-Rays (New York, NY: John Wiley, 1955), 5.

5. G. Kostorz, Neutron Scattering (New York, NY: Academic Press, 1979), Volume 15, p.227.

6. M. Magnani, P. Pulit, and M. Stefanon, to be published.

7. G. D. Wignall and F. S. Bates, "Absolute Calibration of Small-Angle Neutron Scattering Data," J. Appl. Cryst., 10 (1987), 28-40.